

Fermi interaction between the ν_1 and the $\nu_2+4\nu_s$ bands of $\text{Ar}\cdots\text{DN}_2^+$

H. Verbraak

Sackler Laboratory for Astrophysics, Leiden Observatory, Postbus 9513, NL-2300 RA Leiden, The Netherlands

M. Snels

Istituto di Scienze dell' Atmosfera e del Clima, Via Fosso del Cavaliere 100, I-00133 Roma, Italy

P. Botschwina

Institut für Physikalische Chemie, Tammannstrasse 6, D-37077 Göttingen, Germany

H. Linnartz^{a)}

Sackler Laboratory for Astrophysics, Leiden Observatory, Postbus 9513, NL-2300 RA Leiden, The Netherlands

(Received 27 March 2006; accepted 12 April 2006; published online 12 June 2006)

Two rotationally fully resolved vibrational bands have been assigned unambiguously to the linear deuteron bound $\text{Ar}\cdots\text{DN}_2^+$ complex by using ground state combination differences. The ionic complex is formed in a supersonic planar plasma expansion optimized and controlled by a mass spectrometer and is detected in direct absorption using tunable diode lasers and applying production modulation spectroscopy. The band origins are located at 2436.272 cm^{-1} and at 2435.932 cm^{-1} and correspond to the ν_1 band (NN stretch) and to the $\nu_2+4\nu_s$ combination band (DN and intermolecular stretch), respectively. The two bands overlap strongly and the large intensity of the combination band is explained in terms of a Fermi interaction. This interaction perturbs the observed transitions, particularly for low J values. Least-squares fitting yields values for the Fermi interaction parameters of $F_0=0.332\text{ cm}^{-1}$ and $F_J=-0.00146\text{ cm}^{-1}$ and results in accurate rotational constants. These are discussed both from an experimental and a theoretical point of view. © 2006 American Institute of Physics. [DOI: 10.1063/1.2202319]

I. INTRODUCTION

During the past two decades, the investigation of proton-bound ionic complexes by means of rotationally resolved spectroscopy has made significant progress (see Ref. 1 for a review). Many of the complexes studied so far involve rare-gas atoms as binding partners of a molecular cation, with $\text{Ar}\cdots\text{HN}_2^+$ and its isotopomers being the system that has been studied in greatest detail. Most of the current spectroscopic knowledge on $\text{Ar}\cdots\text{HN}_2^+$ and $\text{Ar}\cdots\text{DN}_2^+$ results from infrared (IR) vibrational predissociation²⁻⁴ (PD) and direct absorption⁵⁻⁷ spectroscopy. In addition, pure rotational spectra of six different isotopomers of the ionic complex have been observed by Fourier transform microwave spectroscopy.⁸

IRPD spectroscopy of $\text{Ar}\cdots\text{HN}_2^+$ (Refs. 2 and 3) yielded a remarkably precise value for the dissociation energy ($D_0=2781.5\pm 1.5\text{ cm}^{-1}$) and placed the term value of the lowest accessible excited vibrational state at $2505.40\pm 0.10\text{ cm}^{-1}$. The subsequent analysis of 28 rovibrational transitions in the $2501\text{--}2510\text{ cm}^{-1}$ region, observed by direct IR absorption spectroscopy in a supersonic slit expansion, yielded a more precise value of $\nu_0=2505.4998(4)\text{ cm}^{-1}$.⁵ In both cases, the excited vibrational state was assigned as $\nu_1+\nu_s$, i.e., the combination of one quantum of the stretching vibration of HN_2^+

with highest wave number (ν_1) and one quantum of intermolecular stretching vibration (ν_s). On the basis of coupled cluster calculations at the CCSD(T) level carried out in late 1998,⁹ this assignment had to be revised. Making use of variational calculations with a three-dimensional stretch-only vibrational Hamiltonian, the ν_1 band origin of $\text{Ar}\cdots\text{HN}_2^+$ was predicted at 2519 cm^{-1} .⁶ The corresponding vibration is of mixed character, i.e., may be described as a combination of HN stretching and NN stretching motion, with the latter getting a somewhat larger contribution. This situation is clearly illustrated by a “mass plot” (see Fig. 2 of Ref. 6). The figure shows the harmonic and anharmonic wave numbers of the intramolecular stretching vibrations as a function of the mass of the hydrogen atom, $m_{\text{H}'}$, that is taken as a variable. Within the harmonic approximation, ω_1 shows a strong variation with $m_{\text{H}'}$ in the vicinity of mass 1 u and the harmonic vibration with highest wave number is still predominantly HN stretching in character. The situation changes when anharmonicity effects are taken into account. In this case ν_2 exhibits the strongest variation with $m_{\text{H}'}$. The ν_2 band origin was experimentally determined at $2041.1802(3)\text{ cm}^{-1}$.⁶ The mass plot also demonstrates that the ν_1 and ν_2 bands of $\text{Ar}\cdots\text{DN}_2^+$ have almost local NN and DN stretching characters, respectively. A direct absorption IR spectrum of the latter band ($1593.6058(2)\text{ cm}^{-1}$) was published in 2000 along with the results of CCSD(T) calculations,⁷ which predicted a large transition dipole moment of $|\mu(\nu_2)|=0.541\text{ D}$, only slightly smaller than $|\mu(\nu_2)|=0.611\text{ D}$ as obtained for $\text{Ar}\cdots\text{HN}_2^+$.⁶

^{a)}Author to whom correspondence should be addressed. Fax: +31-71-5275819. Electronic mail: linnartz@strw.leidenuniv.nl

The remaining intramolecular stretching vibration of $\text{Ar}\cdots\text{DN}_2^+$ (ν_1) was calculated to have its origin at 2441 cm^{-1} .⁷ While several earlier searches for this band have been unsuccessful, the band was recently recorded and the results are presented in this work. Surprisingly, not only the ν_1 vibration was found but also a second band that strongly overlaps and that originates from the vibrational ground state of $\text{Ar}\cdots\text{DN}_2^+$ as well. The spectroscopic details are discussed below along with an analysis of the anharmonic interaction between the two modes.

II. EXPERIMENT AND OBSERVATIONS

The experimental setup has been described in detail before.¹⁰ The ionic complexes are produced by electron impact ionization of a gas mixture of Ar, D₂, and N₂ (95:4:1 mixing ratio, stagnation pressure of 550 mbars) that expands through a long and narrow slit of $32\text{ mm}\times 50\text{ }\mu\text{m}$. The electrons are emitted from a heated tungsten wire (1500 K), that is positioned in a slotted molybdenum tube, and are directed towards a slotted metal plate. The tungsten wire and the molybdenum tube are set on a voltage of about -120 V and the metal plate is set on ground potential. In this way the electrons are directed and accelerated towards the expanding gas mixture and upon impact low energetic plasma ignites. In the supersonic expansion rotational temperatures of about 10 K are routinely obtained. The concentration of ions generated in the plasma amounts to about 10^{10} ions/cm^3 . The plasma is sampled by a quadrupole mass spectrometer that is mounted downstream and that allows to optimize the plasma conditions for a particular ionic complex, as several species are produced simultaneously [mainly $\text{Ar}-\text{D}_3^+$, $[\text{Ar}-\text{N}_2]^+$,^{11,12} and $\text{N}_2-\text{D}^+-\text{N}_2$ (Ref. 13)]. Furthermore, the intensity of a mass spectrometric signal can be used to guide an assignment of spectral lines to a specific carrier.

Rotationally resolved spectra are recorded using the radiation of a tunable lead-salt diode laser spectrometer, multipassing the plasma expansion 13 times in a Perry multipass configuration. An étalon and a N₂O reference gas cell are used for relative and absolute calibrations, respectively, yielding an absolute frequency accuracy better than 0.002 cm^{-1} . In order to increase the signal-to-noise ratio, production modulation is used by modulating the voltage over the tungsten wire and molybdenum tube at 12 kHz. This results in an effective plasma modulation and the signal is phase-sensitively detected using lock-in amplifiers.

Guided by previous CCSD(T) calculations⁷ a total of 71 fully rotationally resolved transitions has been recorded in the frequency region between 2432 and 2440 cm^{-1} . The spectrum of the NN stretching vibration being a parallel band of a linear molecule should appear as two distinct series of *P* and *R* transitions, separated by a band gap. The observed spectrum, however, is not that straightforward to interpret as clearly two series of rovibrational transitions overlap. This is demonstrated in Fig. 1 where a typical scan is shown. The two bands overlap and band gaps are not easily identified as the lowest rotational levels are moderately populated at optimal jet conditions. One band—the “broad” band—consists of 44 transitions with *J* values up to 25 in the

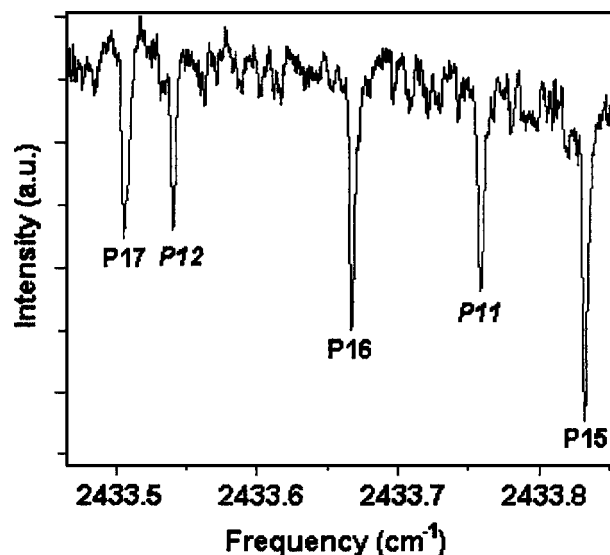


FIG. 1. A typical scan showing part of the *P* branches of the two absorption bands. The lines assigned by italic characters belong to the $\nu_2+4\nu_3$ band, and the normal characters are used for the ν_1 band.

2432 – 2440 cm^{-1} region and the other “narrower” band consists of 27 transitions with *J* values up to 14 in the 2433 – 2437 cm^{-1} region. The latter band converges faster, resulting in a bandhead at rather low *J* values. Even though all signals disappear for plasma without D₂ or N₂ and scale linearly with the $\text{Ar}\cdots\text{DN}_2^+$ mass spectrometric signal, at first hand one does not expect that both bands are due to $\text{Ar}\cdots\text{DN}_2^+$. Both have intensities of comparable magnitude, but it is only the ν_1 fundamental which is expected to show strong absorption signals in this frequency region. Nevertheless, by calculating combination differences $[\Delta_2 F''(J) = R(J-1) - P(J+1)]$ for different *J* assignments and comparing these with the ground state progression as available from the observed ν_2 mode (DN stretch) of $\text{Ar}\cdots\text{DN}_2^+$ around 1593 cm^{-1} ,⁷ the two separate bands are unambiguously assigned as originating from the ground vibrational state of $\text{Ar}\cdots\text{DN}_2^+$. The best average difference of $\Delta_2 F''(J)$ calculated for the two bands presented here and including all observed lines is of the order of 0.0015 cm^{-1} . Alternative numberings result in a much larger average difference.

An overview of all observed transitions is given in Table I. A stick spectrum with the observed line positions and calculated intensities for $T_{\text{rot}}=10\text{ K}$ is shown in Fig. 2.

III. ANALYSIS AND DISCUSSION

Theoretical results for band origins and transition dipole moments of $\text{Ar}\cdots\text{DN}_2^+$ are available from previous work⁷ and the values of interest to the present work are summarized in Table II. The ν_1 band with origin predicted at 2441 cm^{-1} and a relatively large transition dipole moment of 0.234 D is clearly a candidate for the stronger (and broader) of the two observed Σ - Σ -type transitions, while the combination tone $\nu_2+4\nu_3$ may be the carrier of the narrower band. From the variational stretch-only calculations its origin was calculated to be 2408.4 cm^{-1} . This is an underestimate since inclusion of anharmonic stretch-bend interaction, in particular, that between DN stretching and intermolecular bending vibrations,

TABLE I. Observed line positions (cm⁻¹) of rotational transitions in the ν_1 and the $\nu_2+4\nu_s$ bands of Ar...DN₂⁺.

<i>J</i>	ν_1			$\nu_2+4\nu_s$				
	<i>P</i>	o-c ^a	<i>R</i>	<i>P</i>	o-c ^a	<i>R</i>	o-c ^a	
0						2435.8862	-14	
1				2435.5675	-8	2436.0423	-13	
2			2436.9338	2435.4040	-11	2436.1962	-7	
3	2435.9807	22	2437.0725	-17	2435.2383	-12	2436.3484	15
4	2435.8052	7	2437.2159	8	2435.0698	-14	2436.4957	26
5	2435.6272	4	2437.3544	7	2434.8995	-1	2436.6362	14
6	2435.4464	3	2437.4912	3	2434.7246	4	2436.7730	22
7	2435.2626	-5	2437.6185	^b	2434.5442	0	2436.8990	-13
8	2435.0763	-25	2437.7636	-22	2434.3590	4	2437.0203	-17
9	2434.8934	-7	2437.9041	-14	2434.1674	10	2437.1307	-42
10	2434.7089	-14	2438.0475	-5	2433.9674	9	2437.2385	4
11	2434.5275	-9	2438.1924	-13	2433.7584	6	2437.3318	6
12	2434.3474	-18	2438.3423	-8	2433.5397	3	2437.4141	4
13	2434.1721	-13	2438.4958	-4	2433.3116	8		
14	2434.0006	-6	2438.6536	8	2433.0722	5		
15	2433.8321	-5	2438.8138	12				
16	2433.6675	0	2438.9781	27				
17	2433.5064	7	2439.1418	9				
18	2433.3480	11	2439.3117	29				
19	2433.1909	1	2439.4810	21				
20	2433.0398	27	2439.6536	27				
21	2432.8875	20	2439.8279	31				
22			2439.9983	-20				
23	2432.5907	26	2440.1707	-66				
24	2432.4408	-12						
25	2432.2926	-48						

^aObserved-calculated (in 10⁻⁴ cm⁻¹) using the constants shown in Table III.^bNot included in the fit due to poor calibration.

will raise the wave number. A better prediction for the $\nu_2+4\nu_s$ band origin is obtained by adding the calculated difference $(\nu_2+4\nu_s)-\nu_2$ to the experimental value for ν_2 of 1593.6 cm⁻¹.⁷ The result is 2442.6 cm⁻¹, very close to the ν_1 value. In the calculations the latter band is predominantly NN stretching in character and should therefore be only slightly affected by neglecting the stretch-bend interaction. In a reasonably realistic simulation of the anharmonic interaction between vibrational states ν_1 and $\nu_2+4\nu_s$, we may relate the difference $\nu_2(\text{experiment})-\nu_2(\text{CCSD(T)})$ of 34.2 cm⁻¹ to a stretch-bend interaction term Δ_{s-b} as introduced earlier in calculations for free HN₂⁺ and DN₂⁺.¹⁴ In this

way, band origins of 2446.5 cm⁻¹ and 2447.5 cm⁻¹ and transition dipole moments of 0.160 D and 0.174 D are found, respectively.

In the light of the above discussion the observed line positions of the two bands were fitted to a standard $\Sigma-\Sigma$ rovibrational Hamiltonian. The ground state rotational constant B'' has been determined from ground state combination differences (inclusion of the distortion constant D'' did not improve the fit significantly) and the band origins, ν_0 , and excited state rotational constants B' were initially determined using PGOPHER.¹⁵ This, however, did not result in fits that reproduce the observed line positions with an accuracy that

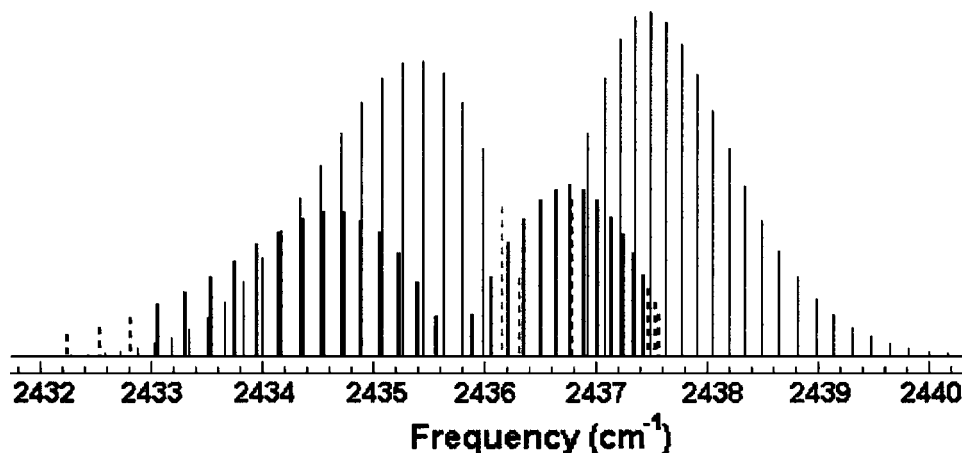


FIG. 2. Stick diagram of the observed line positions with an intensity distribution as typical for $T_{\text{rot}} \sim 10$ K. The dashed lines have not been observed, as signals overlap or are too weak to be detectable.

TABLE II. Predicted and previous experimental wave numbers and transition dipole moments for stretching vibrational transitions of $\text{Ar}\cdots\text{DN}_2^+$.

Band	ν (cm^{-1}) ^a	$ \mu $ (D)
ν_s	195.3	0.384
ν_2	1559.4(1593.6)	0.541
$\nu_2 + \nu_s$	1786.8	0.094
$\nu_2 + 2\nu_s$	2003.7	0.011
$\nu_2 + 3\nu_s$	2210.8	0.001
$\nu_2 + 4\nu_s$	2408.4(2442.6)	0.003
ν_1	2441.0	0.234

^aCCSD(T)/219 cGTO (contracted Gaussian-type orbitals). Values in parentheses are experimental or combined experimental/theoretical values (see text).

is comparable or better than the experimental uncertainty. Clearly, the rovibrational levels are perturbed.

Since both bands have the same symmetry type (both are Σ transitions), it is very likely that the excited state energy levels interact through a Fermi resonance. We therefore explicitly fitted all line positions using a standard Hamiltonian for a rovibrational transition taking into account terms for the Fermi interaction,¹⁶

$$H = \frac{H_1^0 + H_2^0 \pm \sqrt{\delta^2 + 4|H_{12}|^2}}{2}.$$

Here H_1^0 and H_2^0 are the Hamiltonians for the unperturbed rovibrational energies [$H^0 = \nu_0 + B'J(J+1) - D'J^2(J+1)^2$] of the ν_1 and $\nu_2 + 4\nu_s$ modes, respectively, $\delta = H_1^0 - H_2^0$, and $H_{12} = F_0 + F_J J(J+1)$ is the Fermi interaction term. F_0 and F_J are the Fermi interaction parameters for the vibrational and the rotational part of the Hamiltonian, respectively.

Several fits were performed in order to determine which of the molecular constants and the Fermi interaction terms were essential to reproduce the experimental data. The distortion constants D' were set to zero, since their inclusion improved the fit only marginally while causing a large correlation between the fitted parameters. The rotation depen-

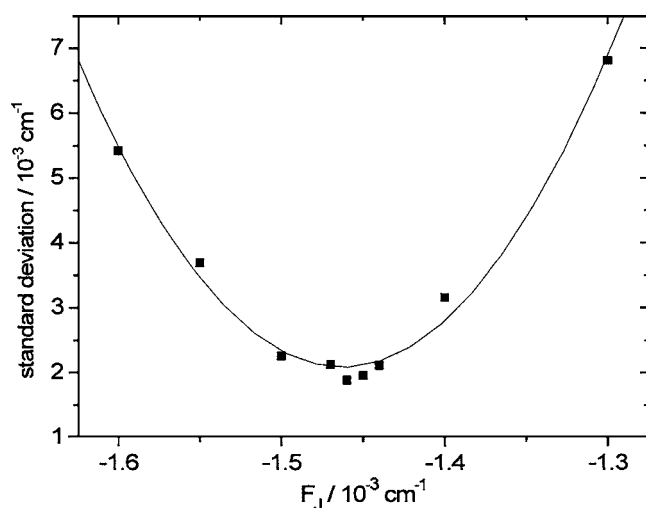


FIG. 3. Standard overall deviation of the fit for a number of fixed F_J values (all other parameters are fitted). The minimum standard deviation corresponds to the parameters reported in Table III, while the errors in Table III correspond to a maximum allowed standard deviation of $4 \times 10^{-3} \text{ cm}^{-1}$.

TABLE III. Experimentally determined constants (cm^{-1}) for the ν_1 and $\nu_2 + 4\nu_s$ bands.

	ν_1	$\nu_2 + 4\nu_s$
ν_0	2436.272(2)	2435.932(5)
B''	0.080 407 ^a	0.080 407 ^a
B'	0.080 28(5)	0.077 09(6)
F_0		0.332(6)
F_J		-0.001 46(11)

^a B'' value taken from ground state combination differences. The uncertainties are derived by explicitly taking into account all fits with a standard deviation of less than $4 \times 10^{-3} \text{ cm}^{-1}$ (see text).

dent part of the Fermi interaction was essential in the fit, but resulted in strong correlation with the other parameters, thereby producing large statistical errors. Therefore we performed a series of least-squares fits, fixing F_J at values between -1.3×10^{-3} and $-1.6 \times 10^{-3} \text{ cm}^{-1}$ and varying all other parameters. The corresponding maximum standard deviations are 6.8×10^{-3} and $5.4 \times 10^{-3} \text{ cm}^{-1}$, respectively, with a minimum value of $1.9 \times 10^{-3} \text{ cm}^{-1}$ at $F_J = -0.001 46 \text{ cm}^{-1}$ (see Fig. 3 for details). This error is close to the estimated experimental error in the line positions. The resulting molecular parameters are summarized in Table III and these values are used to derive the observed-calculated values as listed in Table I. The uncertainties in the fitted parameters, as summarized in Table III, are derived by explicitly taking into account all fits with a standard deviation of less than $4 \times 10^{-3} \text{ cm}^{-1}$.

As can be derived from the red shaded bandhead in the spectrum, the rotational B' constant for the $\nu_2 + 4\nu_s$ state is smaller than the ground state value B'' , resulting in a B''/B' ratio of 1.043. This value is substantially larger than the 0.986–0.991 ratio observed for the ν_1 and ν_2 states (for both $\text{Ar}\cdots\text{HN}_2^+$ and $\text{Ar}\cdots\text{DN}_2^+$) and reflects a substantial stretching upon excitation of four ν_s quanta.

The experimental rotational constants B' given in Table III are in good agreement with the expectations from the previous experimental/theoretical work.⁷ In Table IV the differences of the excited state rotational constants with respect to the corresponding ground state value ($B'' - B'$) are calculated for the four excited states of interest. For the unperturbed ν_1 state, the results of coupled cluster calculations with two different basis sets (219 and 368 cGTOs, respectively) result in a value of $-0.000 34 \text{ cm}^{-1}$. The corresponding experimental value from the present work is

TABLE IV. Predicted and experimental rotational constant differences for stretching vibrational states of $\text{Ar}\cdots\text{DN}_2^+$.

Excited state	$B'' - B'$		Experiment
	CCSD(T)/219cGTO	CCSD(T)/368 cGTO	
ν_s (inter stretch)	0.001 08	0.000 99	
ν_2 (\sim DN stretch)	-0.001 60	-0.001 68	-0.000 76
$\nu_2 + 4\nu_s$	0.002 72	0.002 28	0.003 32
	(0.003 56) ^a	(0.003 20) ^a	
ν_1 (\sim NN stretch)	-0.000 34	-0.000 34	0.000 13

^aSee text for explanation.

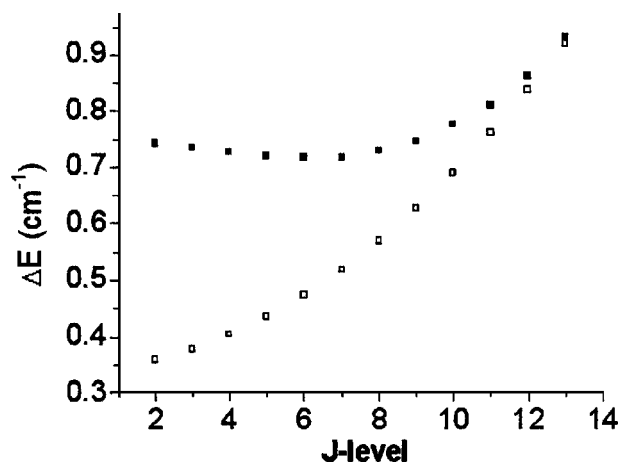


FIG. 4. Difference in energy between the ν_1 band and the $\nu_2+4\nu_s$ band for each J level ($\Delta E = E_{\nu_1}(\nu, J) - E_{\nu_2+4\nu_s}(\nu, J)$); (■) show the differences, in which both states are perturbed, while (□) show the differences, in which both bands are unperturbed.

0.000 13 cm^{-1} . The small mismatch is due to the fact that the theoretical values are obtained from conventional second order perturbation theory in normal coordinate space which is well known to have limitations for systems with a high degree of vibrational anharmonicity. The CCSD(T) results for the $\nu_2+4\nu_s$ state are obtained from the values reported for α_2 and α_s in Ref. 7. This yields 0.002 72 cm^{-1} and 0.002 28 cm^{-1} and becomes 0.003 56 cm^{-1} and 0.003 20 cm^{-1} when the experimental value for α_2 is used.⁷ The latter two values are in excellent agreement with the corresponding experimental value of 0.003 32 cm^{-1} (Table III).

The Fermi interaction term F_0 is comparable to the difference of the two unperturbed vibrational energy levels ($\delta = 2436.272 - 2435.932 = 0.340 \text{ cm}^{-1}$), which means that the intensity borrowing is rather efficient. This can easily be deduced from the formula for the relative intensity of two bands,¹⁶

$$\frac{I_1}{I_2} = \frac{\sqrt{4H_{12}^2 + \delta^2} - \delta}{\sqrt{4H_{12}^2 + \delta^2} + \delta} = 0.37 \quad \text{for } J=0.$$

In this case the perturbation has a strong rotational character which implies that the total interaction term $[F_0 + J(J+1)F_J]$ vanishes for $J=15$. This is in good agreement with the observations, since no lines of the combination band have been observed for J greater than 14, even though these are expected for a rotational temperature of 10 K. This is also demonstrated in Fig. 4. Here the energy differences $\Delta E = E_{\nu_1}(\nu, J) - E_{\nu_2+4\nu_s}(\nu, J)$ ($= P(J+1)_{\nu_1} - P(J+1)_{\nu_2+4\nu_s} = R(J-1)_{\nu_1} - R(J-1)_{\nu_2+4\nu_s}$) between the two perturbed vibrations for each J level are displayed as filled squares and are calculated from the observed transitions (Table I). The open squares show the (unperturbed) ΔE values calculated from the rotational constants as listed in Table III excluding the Fermi interaction parameters. Figure 4 shows that the perturbation (which occurs between energy levels of the same angular momentum J) is stronger for lower J . This is due to the rotational dependence of the interaction Hamiltonian and to the increasing energy separation with J for the two vibra-

tional energy levels. It is obvious from the figure that the strength of the perturbation depends on the value of the J level and gets weaker with increasing values of J .

IV. CONCLUSIONS

Following earlier theoretical predictions,^{6,7} the ν_1 band of Ar...DN₂⁺ could finally be detected in direct absorption using tunable diode laser spectroscopy. Calculated and experimental band origins differ by only 5 cm^{-1} . The ν_1 band is found to undergo accidental anharmonic interaction of higher order with the combination tone $\nu_2+4\nu_s$. Deperturbed rotational constants of the two excited vibrational states agree nicely with the predictions that can be made on the basis of an earlier joint experimental/theoretical study.⁷ According to the mass plot published in Fig. 2 of Ref. 6, the unperturbed ν_1 band corresponds predominantly to a NN stretching vibration. Compared with free DN₂⁺, where the ν_3 band with observed origin at 2024.04 cm^{-1} (Refs. 17 and 18) is mostly NN stretching in character, an increase in wave number by as much as 412.3 cm^{-1} is observed. Using the harmonic wave number ω_1 from the CCSD(T) calculations with the large basis set of 368 cGTOs,⁷ the anharmonicity contribution to ν_1 is 91 cm^{-1} , much smaller than the corresponding value of 278 cm^{-1} obtained for Ar...HN₂⁺.⁶ On the other hand, formation of the Ar...DN₂⁺ complex is connected with a large redshift of the DN stretching vibration ν_2 [1043.4 cm^{-1} with respect to free DN₂⁺ (Ref. 19)]. The ν_2 band lies well below the ν_1 band and exhibits an anharmonicity contribution of 149 cm^{-1} .

ACKNOWLEDGMENTS

The authors thank the Netherlands Organization for Scientific Research (NWO) through FOM (Dutch Organization for Fundamental Research). Financial support from the top research school NOVA is gratefully acknowledged. The Laser Centre of the Free University Amsterdam (LCVU) is thanked for substantial instrumental support. One of the authors (M.S.) also acknowledges EU support within the integrating infrastructure initiative, Contract No. RII3-CT-2003-506350. Another author (P.B.) gratefully appreciates support from the Fonds der Chemischen Industrie. We thank Professor Luciano Fusina for very helpful discussions. Special thanks go to Laser Components for making available a number of diodes to cover the frequency regime studied here.

¹E. J. Bieske and O. Dopfer, Chem. Rev. **100**, 3963 (2000).

²S. A. Nizkorodov, Y. Spinelli, E. J. Bieske, J. P. Maier, and O. Dopfer, Chem. Phys. Lett. **265**, 303 (1997).

³S. A. Nizkorodov, Ph.D. thesis, University of Basel, 1997.

⁴O. Dopfer, R. V. Olkhov, and J. P. Maier, J. Phys. Chem. A **103**, 2982 (1999).

⁵T. Speck, H. Linnartz, and J. P. Maier, J. Chem. Phys. **107**, 8706 (1997).

⁶P. Botschwina, R. Oswald, H. Linnartz, and D. Verdes, J. Chem. Phys. **113**, 2736 (2000).

⁷D. Verdes, H. Linnartz, and P. Botschwina, Chem. Phys. Lett. **329**, 228 (2000).

⁸K. Seki, Y. Sumiyoshi, and Y. Endo, J. Chem. Phys. **117**, 9750 (2002).

⁹P. Botschwina and R. Oswald, Conference on Electron Correlation in Spectroscopy and Dynamics, Kaiserslautern, 1998 (unpublished), Poster P38.

¹⁰H. Linnartz, D. Verdes, and T. Speck, Rev. Sci. Instrum. **71**, 1811 (2000).

¹¹H. Linnartz, D. Verdes, and J. P. Maier, Science **297**, 1166 (2002).

- ¹²H. Verbraak, J. N. P. van Stralen, J. Bouwman, J. S. de Klerk, D. Verdes, H. Linnartz, and F. M. Bickelhaupt, *J. Chem. Phys.* **123**, 144305 (2005).
- ¹³D. Verdes, H. Linnartz, J. P. Maier, P. Botschwina, R. Oswald, P. Rosmus, and P. J. Knowles, *J. Chem. Phys.* **111**, 8400 (1999).
- ¹⁴P. Botschwina, *Chem. Phys. Lett.* **107**, 535 (1984).
- ¹⁵C. M. Western, PGOPHER, a program for simulating rotational structure, University of Bristol, <http://pgopher.chm.bris.ac.uk>
- ¹⁶C. H. Townes and A. L. Schawlow, *Microwave Spectroscopy* (Dover, New York, 1975).
- ¹⁷S. C. Foster and A. R. W. McKellar, *J. Chem. Phys.* **81**, 3424 (1984).
- ¹⁸J. W. Owrutsky, C. S. Gudeman, C. C. Martner, L. M. Tack, N. H. Rosenbaum, and R. J. Saykally, *J. Chem. Phys.* **84**, 605 (1986).
- ¹⁹D. J. Nesbitt, H. Petek, C. S. Moore, and R. J. Saykally, *J. Chem. Phys.* **81**, 5281 (1984).